

Tyrosyl-DNA-phosphodiesterase I (TDP1) participates in the removal and repair of stabilized-Top2 α cleavage complexes in human cells

Miguel Angel Borda ¹, Micaela Palmitelli ¹, Gustavo Verón, Marcela González-Cid, Marcelo de Campos Nebel *

Laboratorio de Mutagénesis, Instituto de Medicina Experimental (CONICET-Academia Nacional de Medicina), Buenos Aires, Argentina



ARTICLE INFO

Article history:

Received 19 January 2015

Received in revised form 21 August 2015

Accepted 11 September 2015

Available online 14 September 2015

Keywords:

Topoisomerase II-mediated DNA damage

DNA double strand break repair

Tyrosyl-DNA-phosphodiesterase I

Genome instability

ABSTRACT

Tyrosyl-DNA-phosphodiesterase 1 (TDP1) is a DNA repair enzyme that removes irreversible protein-linked 3' DNA complexes, 3' phosphoglycolates, alkylation damage-induced DNA breaks, and 3' deoxyribose nucleosides. In addition to its extended spectrum of substrates, TDP1 interacts with several DNA damage response factors. To determine whether TDP1 participates in the repair of topoisomerase II (Top2) induced DNA lesions, we generated TDP1 depleted (TDP1kd) human tumoral cells. We found that TDP1kd cells are hypersensitive to etoposide (ETO). Moreover, we established in a chromatin context that following treatment with ETO, TDP1kd cells accumulate increased amounts of Top2 α cleavage complexes, removing them with an altered kinetics. We also showed that TDP1 depleted cells accumulate increased γ H2AX and pS296Chk1 signals following treatment with ETO. Similarly, cytogenetics analyses following Top2 poisoning revealed increased amounts of chromatid and chromosome breaks and exchanges on TDP1kd cells in the presence or not of the DNA-PKcs inhibitor NU7026. However, the levels of sister chromatid exchanges were similar in both TDP1kd and control non-silenced cell lines. This suggests a role of TDP1 in both canonical non-homologous end joining and alternative end joining, but not in the homologous recombination repair pathway. Finally, micronucleus analyses following ETO treatment revealed a higher frequency of micronucleus containing γ H2AX signals on TDP1kd cells. Together, our results highlight an active role of TDP1 in the repair of Top2-induced DNA damage and its relevance on the genome stability maintenance in human cells.

© 2015 Elsevier B.V. All rights reserved.

1. Introduction

DNA topoisomerases are ubiquitous and essential enzymes that relieve torsional stress, playing a central role in almost every metabolic process of DNA [1]. In mammals, topoisomerase II (Top2) has two isoforms, Top2 α and Top2 β , which are coded by different genes and show different expression patterns in proliferating and terminally differentiated cells [2,3]. Homodimeric Top2 catalyzes the passage of a duplex from the same or a different molecule

through a transient double-stranded break (DSB) generated in the DNA. Each Top2 monomer cleaves the phosphodiester backbone of a DNA strand by a nucleophilic attack from a catalytic tyrosine residue, becoming linked to a 5' phosphate end of the DNA break [4]. These catalytic intermediates, termed Top2 cleavage complexes (Top2cc), are rapidly reverted and do not represent a threat for the integrity of the genome. However, several endogenous [5–8] and exogenous [9–11] factors, including the chemotherapeutic agents etoposide (ETO), have the ability to trap the Top2cc, increasing their half-life and thus, the likelihood of collision with either the replication or transcriptional machineries. Further nucleolytic/proteolytic processing steps of the stabilized Top2cc, allow the recognition of the resulting Top2 peptide-bound 5' ends of the DNA as true DSB [12,13].

In response to DNA DSB, the cells activate the DNA damage response (DDR), which involves chromatin remodeling, check-

* Corresponding author at: Laboratorio de Mutagénesis, Instituto de Medicina Experimental (CONICET-Academia Nacional de Medicina), J.A. Pacheco de Melo 3081, Buenos Aires 1425, Argentina. Fax: +54 11 4803 9475.

E-mail address: mnebel@hematologia.ann.edu.ar (M. de Campos Nebel).

1 These authors contributed equally to this article.

point activation and DNA repair [14]. The proteins ATM (Ataxia telangiectase mutated), ATR (Ataxia telangiectase mutated/Rad3 related), and DNA-PKcs (DNA-dependent Protein kinase catalytic subunit) are key DDR components. While ATM-CHK2 (Checkpoint kinase 2) are rapidly activated by DSBs, ATR-CHK1 (Checkpoint kinase 1) is classically activated by single stranded DNA regions arising as a result of replication stress and following later resection of DSBs. CHK1 and CHK2 are both required for the proper activation and maintenance of G2/M checkpoint [15].

In proliferating human somatic cells, two major DNA DSB repair pathways are homologous recombination (HR) and canonical non-homologous end joining (C-NHEJ) [16,17]. In addition, an alternative end joining (A-EJ) process has also been reported [18], which is strongly restricted by the activity of C-NHEJ [19] and probably by the HR activity as well.

Human tyrosyl-DNA phosphodiesterase 1 (TDP1) is a nuclear and mitochondrial DNA repair enzyme [20] which is associated to the autosomal recessive disorder spinocerebellar ataxia with axonal neuropathy (SCAN1). SCAN1 phenotype results from the failure to repair DNA-protein covalent complexes [21]. TDP1 has the ability to process several blocking-end structures, such as Top1-mediated 3' phosphotyrosyl DNA ends, 3' deoxyribose phosphates from the hydrolysis of abasic sites, alkylation base damage, and 3' phosphoglycolates [22–25]. Despite its polarity, yeast tdp1 has also been implicated in the repair of Top2cc [26]. However, the participation of vertebrate TDP1 in the repair of Top2cc has been controversial [22,27–29].

Here we show by using human tumoral TDP1 depleted cells that TDP1 participates of the removal of Top2αcc, in a chromatin context, although it is unessential in that function. Moreover, we demonstrate that cells with TDP1 knocked down accumulate DSB, increase CHK1 activation and genome instability following Top2-mediated DNA damage. These findings are consistent with a role of TDP1 in both C-NHEJ and A-EJ pathways of DSB repair.

2. Materials and methods

2.1. Reagents

ETO (CAS no. 33419-42-0; Sigma), NU7026 (CAS no. 154447-35-5; Calbiochem) and KU55933 (CAS no. 587871-26-9; Santa Cruz) were dissolved in DMSO. Bromodeoxyuridine (BrdU; CAS no. 59-14-3; Sigma), Puromycin (CAS no. 58-58-2; Sigma) and TCS2312 (CAS no. 838823-32-8; Santa Cruz) were dissolved in bidistilled water.

2.2. Cell cultures, TDP1 knockdown and drug treatments

The human HeLa cell line was kindly provided by Dr. María Cecilia Carreras (INIGEM-UBA, Hospital de Clínicas “José de San Martín”, Ciudad Autónoma de Buenos Aires, Argentina) and was grown in RPMI 1640 supplemented with 10% FBS and 2 mM L-glutamine and antibiotics (complete media). All the cell cultures were incubated at 37 °C under a 5% CO₂ humidified atmosphere.

HeLa cells were transfected with pGIPZ human TDP1sh-1 (Open Biosystems, clone id: V2LHS-174999, RHS4430-98818285) or pGIPZ TDP1sh-2 (Open Biosystems, V3LHS-300804, RHS4430-101066291) or pGIPZ Non-Silencing (NS) shRNA control (Open Biosystems, #RHS4346) using Lipofectamine 2000 (Invitrogen) according to manufacturer's instructions. After 48 h, the cells were grown in selection medium containing puromycin 1 µg/ml which was renewed every third day. The selection process was performed by 3–4 weeks and clonal selection of stable transfectants was carried out. Clone TDP1sh-2 from Supplementary Fig. S1 was termed

HeLa TDP1kd and the non-silencing control HeLa NS. The level of knockdown was monitored by qRT-PCR and western blot.

HeLa, HeLa TDP1kd or HeLa NS cell lines were treated with different doses of ETO and by different lapses of time as specified in the text or figures.

2.3. Quantitative real-time RT-PCR

RNA from HeLa TDP1kd and NS cell lines was extracted using the TRIzol (Ambion) method and RNA concentration determined by spectrophotometry. Total RNA (1 µg/reaction) was reverse-transcribed using random primers (Biodynamics) and M-MLV enzyme (Promega). Real time PCR analysis was performed with “Mezcla Real” reaction mix (Biodynamics) in a RotorGene thermocycler (QIAGEN). The primers for amplifying human TDP1 (FW: 5'-ATCCTGCTCCAATGAC-3', RV: 5'-GGCTTCTTCGAACTCTG-3') and TDP2 (FW: 5'-GCCTTATGACATCCCATTGGA-3', RV: 5'-GGTAACCTCTCGATCCCTTAGAT-3') and ACTB (FW: 5'-CAGAGGCTTACAGGGATAG-3', RV: 5'-CCAACCGCGAGAAGATGA-3') were from Genbiotech. The human ACTB gene was used as reference. The percentage of TDP1 mRNA reduction and TDP2 expression was estimated based on the relative expression ratio with ACTB according to Pfaffl method [30].

2.4. Cell proliferation rates and clonogenic survival

HeLa TDP1kd and NS cells (3×10^4 /well) were seeded in 12-well plates in complete media and harvested after 24, 48, 72 or 96 h. The cells were resuspended in 1 ml of PBS and an aliquot of each cell suspension was diluted in equal parts with a 0.4% Trypan blue solution. The total number of viable cells/ml for each culture was calculated by visual scoring in a Neubauer chamber.

For colony assay, HeLa TDP1kd and NS cells were plated at low density (300–600 cells/dish), allowed to attach for 6 h, and treated with different concentrations of ETO for 20 h. The cells were then washed with PBS and cultured in fresh complete media for 10–14 days. After this growth period, the cells were rinsed with PBS, fixed with methanol 100%, and stained with crystal violet. Colonies containing more than 50 cells were scored. Survival fraction was estimated as the ratio of colonies in ETO-treated cultures compared with control cultures and expressed in percentages. Three to four independent experiments were carried out for each end point.

2.5. Immunoblot

Whole cell extracts were prepared in RIPA buffer (50 mM Tris-HCl pH 7.0, 150 mM NaCl, 1% NP-40, 0.5% sodium deoxycolate and 0.1% SDS) containing a cocktail of protease inhibitors and the protein concentrations were determined by the Bradford method [31]. Eighty microgram of total proteins were separated on 6% or 8% SDS-PAGE and transferred onto PVDF membranes. After an overnight blocking step in 0.2% Tween20/PBS containing 5% non-fat dry milk, the membranes were incubated for 2 h with primary antibodies. The following monoclonal antibodies: anti Top2b (1:500, Santa Cruz), anti HDAC1 (1:1000, Cell Signaling), anti pS1981ATM (1:1000, Santa Cruz); and polyclonal antibodies: anti Top2a (1:500, Santa Cruz), anti TDP1 (1:1000, Abcam), anti ATM (1:1000, Calbiochem), anti pS2056DNA-PKcs (1:1000, Abcam), anti pS428ATR (1:1000, Cell Signaling), anti pS296CHK1 (1:1000, Cell Signaling), anti pT68CHK2 (1:1000, Cell Signaling), and anti RAD51 (1:1000, Santa Cruz) were used. Appropriated HRP-conjugated anti mouse or anti rabbit antibodies (1:10000) and the ECL kit (Amersham) were used for protein detection by autoradiography.

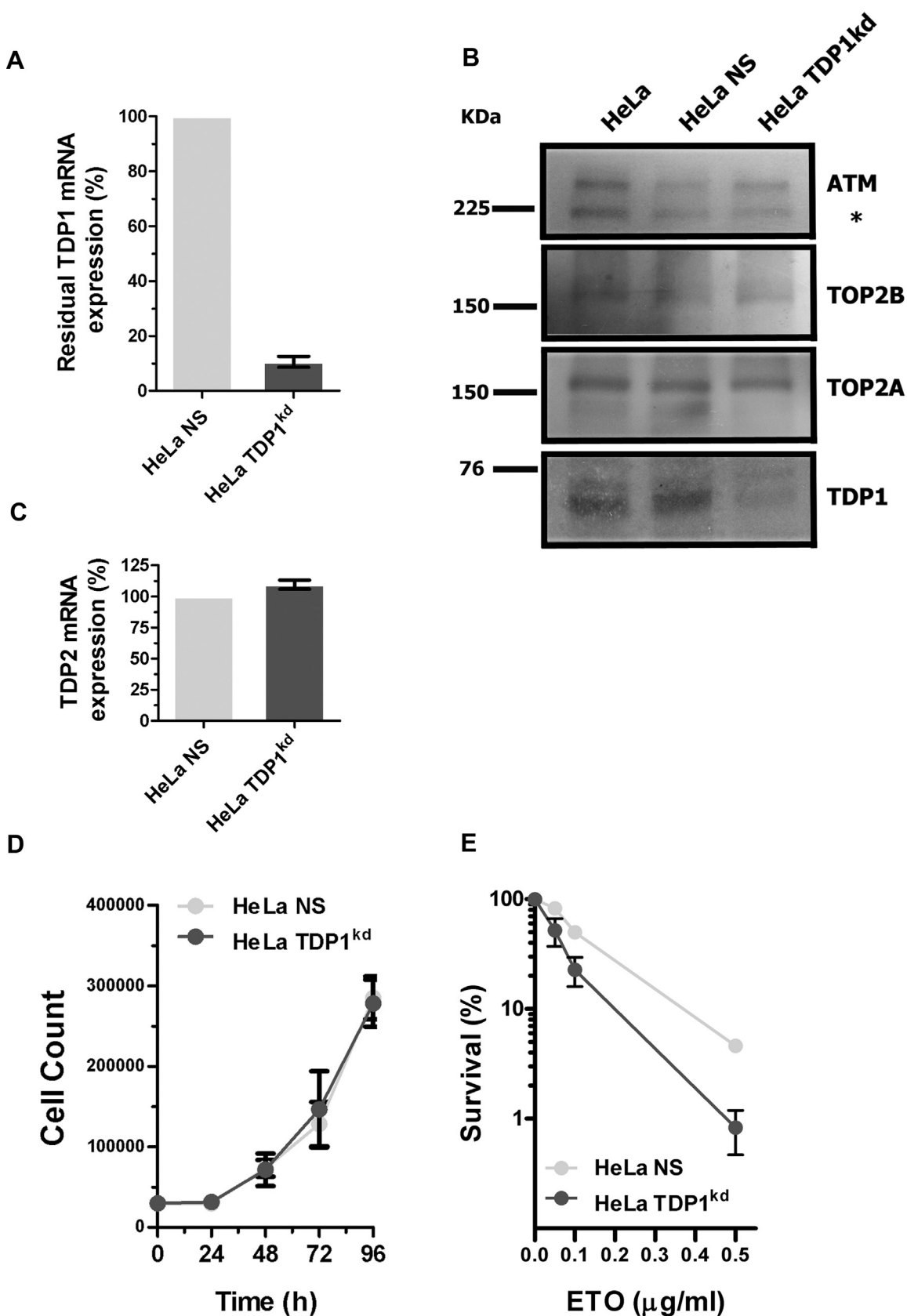


Fig. 1. HeLa TDP1^{kd} cells show normal proliferation rates and increased sensitivity to ETO. Analyses of TDP1 expression by (A) qRT-PCR and (B) western blot. *Unspecific band. (C) Analyses of TDP2 expression by qRT-PCR. (D) HeLa TDP1^{kd} and NS cells show similar proliferation rates. (E) Clonogenic survival of HeLa TDP1^{kd} and NS cells following treatment with ETO 0, 0.05, 0.1 or 0.5 μg/ml for 20 h. Error bars in (A), (C), and (E) indicate s.e.m. Error bars in (D) indicate s.d.

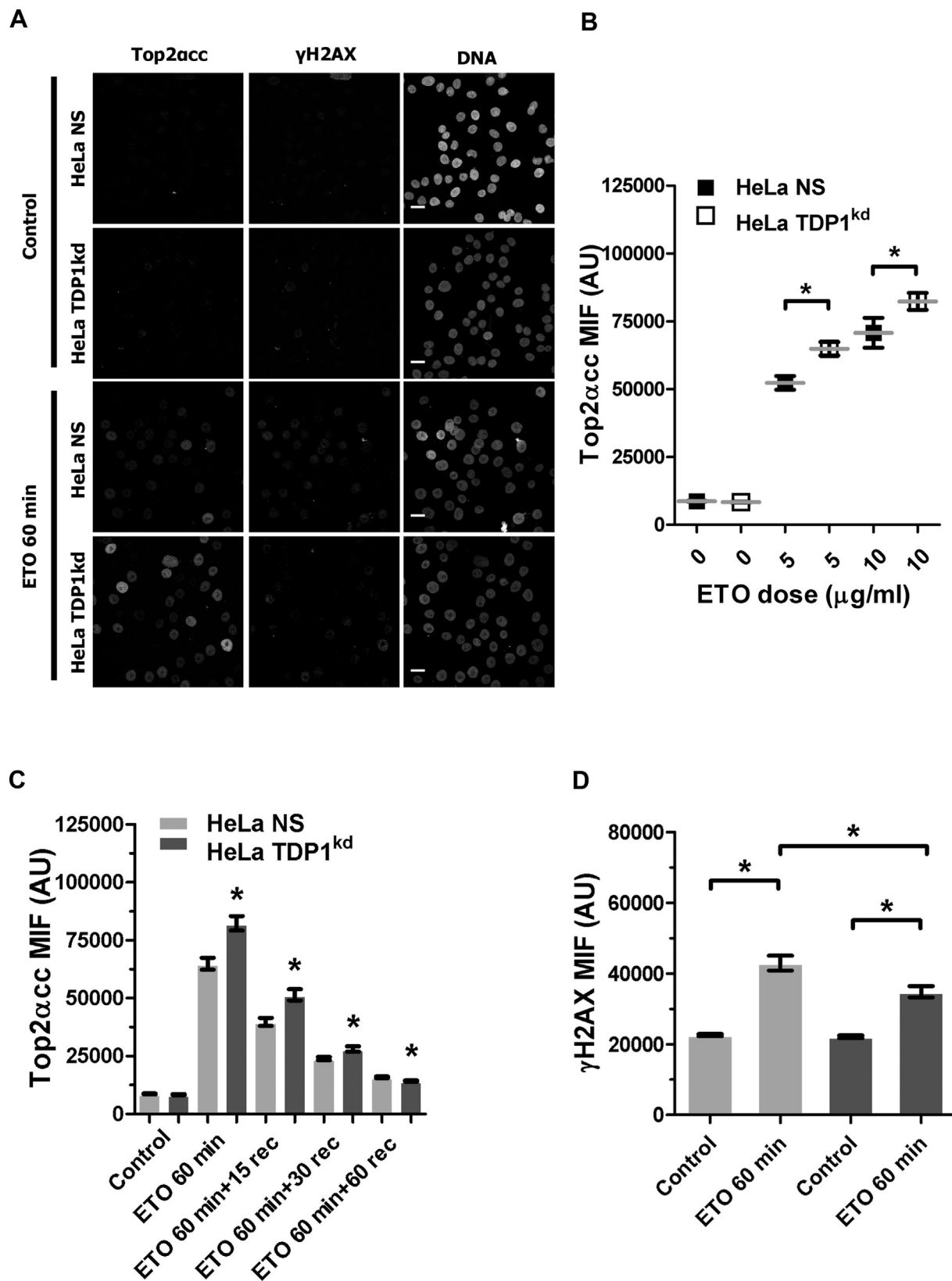


Fig. 2. ETO-stabilized Top2 α cleavage complexes (Top2 α cc) accumulate in HeLa TDP1kd cells. (A) Maximal intensity projections images following DRT assay of HeLa NS and TDP1kd cells showing Top2 α cc and γ H2AX nuclear signals in control and ETO 10 μ g/ml for 60 min. Scale bar = 20 μ m. (B) Top2 α cc formation following 1 h treatment with different dose of ETO in HeLa TDP1kd and NS cells. * p < 0.05 (Student t -test). (C) Kinetics of Top2 α cc formation and removal at different recovery times (rec) in HeLa NS and TDP1kd cells. * p < 0.05 (compared to HeLa NS cells, Student t -test). (D) HeLa TDP1kd cells showed diminished γ H2AX signals at the time of maximal accumulation of Top2 α cc compared to NS cells. * p < 0.05 (Student t -test). MIF—median intensity of fluorescence. AU—arbitrary units. Error bars indicate s.e.m.

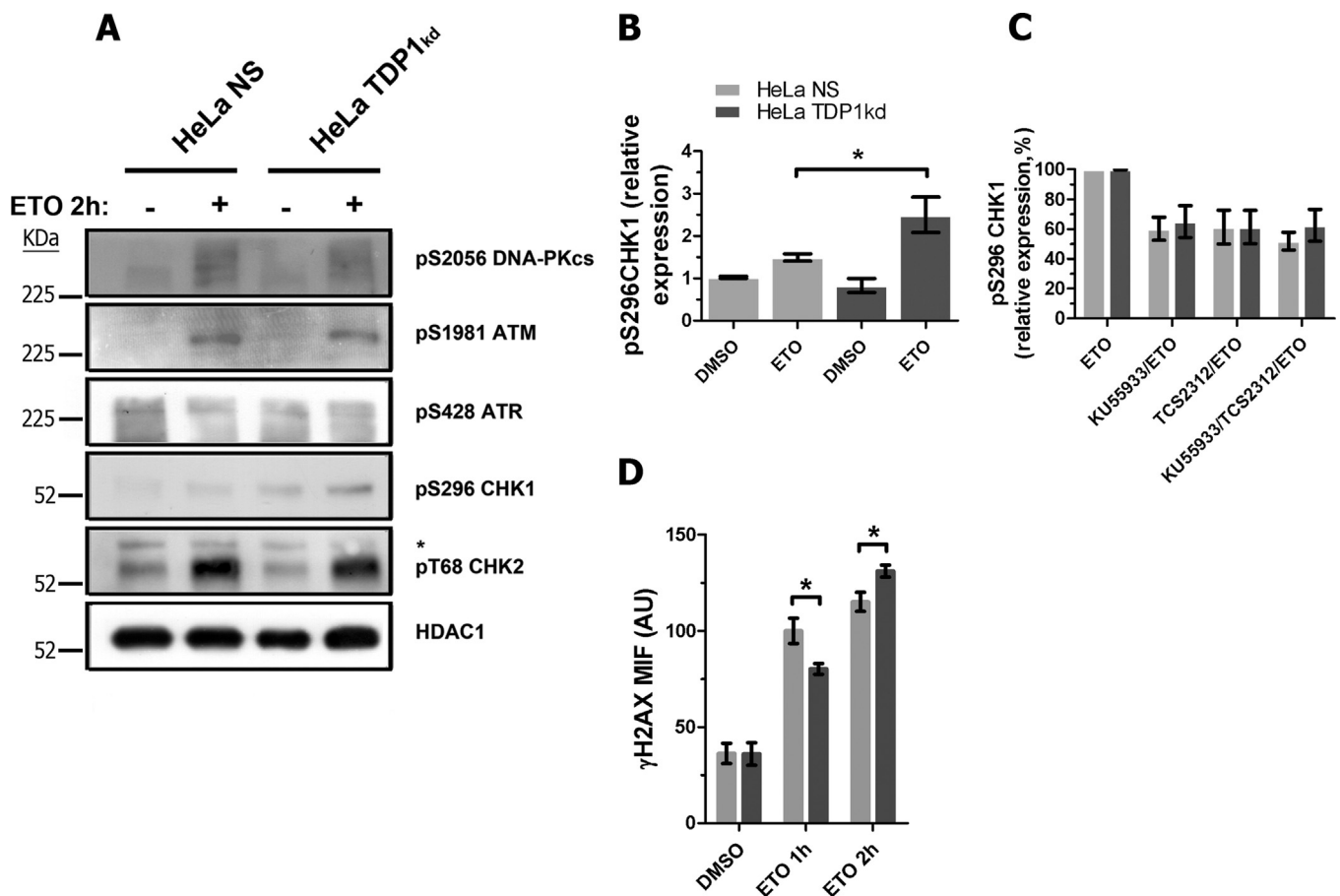


Fig. 3. Top2-induced DNA damage signaling in TDP1 depleted cells. (A) Western blot analyses of proximal (pS2056DNA-PKcs, pS1981ATM, pS428ATR) and distal (pS296CHK1 and pT68CHK2) transducers in HeLa NS and TDP1kd cells following a 2 h treatment with ETO 10 µg/ml. HDAC1 was used as loading control. (B) pS296CHK1 expression levels are increased in HeLa TDP1kd respect to NS following 2 h treatment with ETO 10 µg/ml. (C) pS296CHK1 levels are similarly diminished on HeLa NS and TDP1kd cells following pre-incubation by 30 min with the ATM inhibitor KU55933 10 µM, the CHK1 inhibitor TCS2312 3 µM, or both before the treatment by 2 h with ETO 10 µg/ml. The inhibitors were present in the culture during the whole treatment. (D) Levels of γH2AX analyzed by flow cytometry in HeLa NS and TDP1kd cells following 1 h or 2 h treatment with ETO 10 µg/ml. MIF—median intensity of fluorescence. AU—arbitrary units. * $p < 0.05$ (Student *t*-test). Error bars indicate s.e.m.

2.6. DRT assay and immunofluorescence

The differential retention of topoisomerase II (DRT) assay was performed as reported by Agostinho et al. [32] with minor modifications. Briefly, 5×10^5 HeLa TDP1kd or NS cells growing on coverslides were treated with ETO 10 µg/ml for 60 min or treated and allowed to recover in drug-free complete media for 15, 30 or 60 min. Control cultures were treated with DMSO 0.5% for 60 min. Cells were rinsed in cold PBS and then extracted on ice, with gentle agitation, for 2 min in PHEM buffer (65 mM Pipes, 30 mM HEPES, 10 mM EGTA, 2 mM Mg₂Cl, pH 6.9) supplemented with 350 mM NaCl, 0.5% Triton X-100, and 1 mM PMSF. Cells were then fixed with 2% paraformaldehyde in PHEM buffer for 15 min at room temperature before immunolabeling. Samples were then blocked (3% BSA, 0.25% Triton X-100 in PBS) for 1 h, followed by incubation for 2 h with rabbit anti Top2a (1:250, Santa Cruz) or mouse anti γH2AX (1:500; Upstate; clone JBW301). Secondary Alexa Fluor 488-conjugated anti-rabbit (1:200, Life Technologies) or Texas Red-conjugated anti-mouse (1:250, Vector Laboratories) antibodies were used. Images were acquired using a Fluoview FV1000 confocal microscope (Olympus) equipped with a PlanApo 60X/1.42 objective lens and processed using FV10-ASW software (Olympus) or ImageJ (NIH) Software packages. Z-stack images covering the whole nuclear volume were captured and the total intensity of flu-

orescence quantified using the ImageJ software. Two hundred cells from each cell line and time point were analyzed. Three to four independent experiments were performed.

For Rad51 foci formation studies, the fixation and permeabilization process was performed in 2% paraformaldehyde containing 0.25% Triton X-100 in PBS for 15 min, and continued as mentioned above. The rabbit anti RAD51 (1:200, Santa Cruz) antibody was used. The RAD51 foci number per nucleus was quantified by manual scoring of at least 300 cells per treatment, from three independent experiments.

2.7. Flow cytometry

For flow cytometry analysis of γH2AX, cellular suspensions were fixed with 1% paraformaldehyde in PBS and permeabilized in 0.25% Triton X-100 in PBS, and then processed for immunolabeling as specified in Section 2.6. Thirty-thousand cells per sample were evaluated and the experiments were performed thrice.

2.8. Chromosomal aberrations and mitotic index

Cell lines were plated in 60 mm dishes, and treated with ETO for 2 h. Cultures were then washed twice with PBS and incubated in fresh complete media for 20 h. To analyze the participation of A-EJ

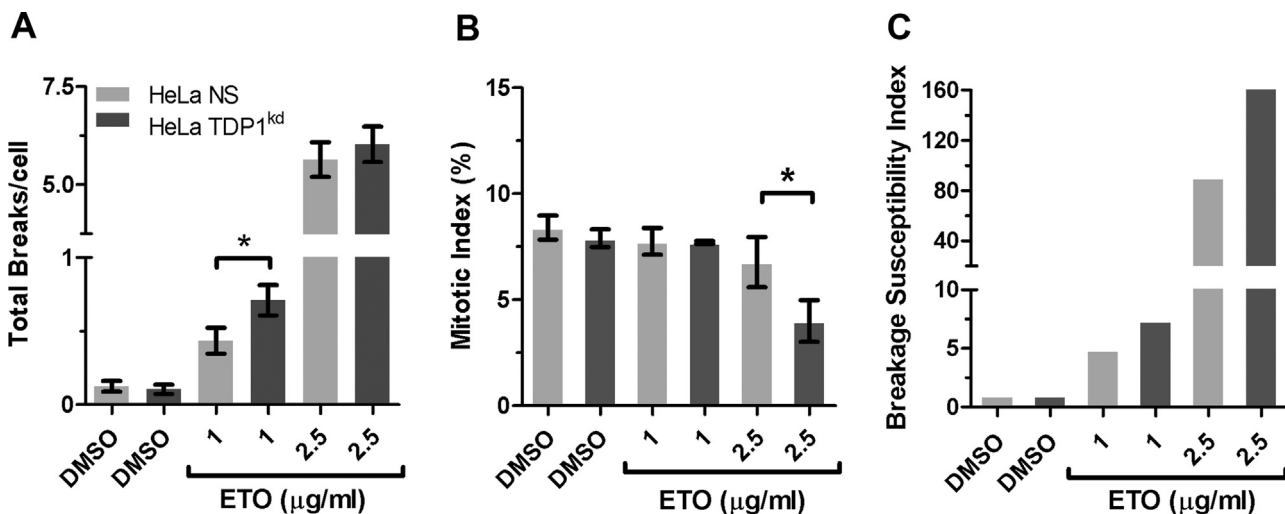


Fig. 4. TDP1 participates in the repair of Top2-mediated DNA DSB. (A) Total DNA breaks analyses of HeLa NS and TDP1^{kd} chromosome spreads following treatments with different doses of ETO for 2 h. Error bars indicate s.e.m. (B) Mitotic index analyses following the different doses of ETO for 2 h. Error bars indicate s.d. (C) Breakage susceptibility index for the different doses of ETO, which reflects both the increased total breaks and the inhibition of the mitotic index. * $p < 0.05$ (Student *t*-test).

repair pathway, cells were pretreated with NU7026 10 μ M for 1 h, coincubated with ETO for 2 h and kept in media containing NU7026 for the remaining culture time (20 h). Colcemid (0.1 μ g/ml) was added 1.5 h before harvesting, and then, cells were trypsinized and collected by centrifugation. Cells were exposed to hypotonic solution 0.075 M KCl, fixed in methanol:acetic acid (3:1) and stained with 10% Giemsa for 4 min. For each treatment, 200 metaphases containing 66 ± 3 chromosomes were analyzed for the induction of chromosomal aberrations (CA). The gaps were excluded from the analysis of CA frequencies.

Aberrations were classified as chromosome and chromatid breaks, and chromosome and chromatid exchanges. Complete and incomplete chromatid exchanges and intrachanges in the same configuration were considered as complex exchange configurations. For the quantification of total breaks, chromatid and chromosome breaks were scored as one break and quadriradial and triradial chromosome configurations, dicentric and rings chromosomes were scored as two breaks. Mitotic index (MI) was calculated as the number of metaphases among 1000 nuclei. Breakage susceptibility index for each cell line was estimated as follow: (mean value of total breaks in ETO treatment/mean value of total breaks in control) \times (1 – fraction of MI in ETO treatment/1 – fraction of MI in control). Two to 4 independent experiments were performed for each end point.

2.9. Sister chromatid exchanges (SCE)

HeLa NS and TDP1^{kd} cells were treated by 2 h with ETO and then incubated with 10 μ g/ml BrdU for two complete rounds of replication (~ 44 h). The SCE average was taken from the analysis of 30 metaphases during the second cycle of division in 3 independent experiments.

2.10. γ H2AX detection on micronucleated cells

HeLa TDP1^{kd} or NS cells growing on coverslips were treated with ETO for 2 h. The cells were washed and cultured in complete media for an additional 20 or 36 h. Samples were fixed and permeabilized in 1% paraformaldehyde containing 0.25% Triton X-100/PBS at room temperature for 20 min. Samples were then immunolabeled with anti γ H2AX as described in Section 2.6. The

frequency of micronuclei and main nuclei containing γ H2AX foci were determined by analyzing at least 1000 cells per sample. Three independent experiments have been scored.

3. Results

3.1. TDP1 knockdown human cells are hypersensitive to ETO

Following the selection of stably transfected HeLa cells with a non-silencing (NS) or a specific shRNAmir sequence against TDP1, we analyzed the expression of TDP1. As shown in Fig. 1A, the relative expression levels of TDP1 mRNA was decreased by a 90% in HeLa TDP1^{kd} compared to HeLa NS. To confirm that this effect correlates with a reduced protein expression, we analyzed TDP1 protein by western blot. Fig. 1B (and also Supplementary Fig. S1A) shows that levels of TDP1 protein were also diminished in HeLa TDP1^{kd} as compared to HeLa NS or the non-transfected cell line, while other nuclear proteins such as ATM, Top2 α and Top2 β remained at similar levels. The analysis of TDP2 mRNA expression showed small but not significant increase (~8%) in TDP1^{kd} compared to NS cells (Fig. 1C). In addition, we evaluated the cellular proliferation rates (Fig. 1D) of both HeLa NS and TDP1^{kd}. We found that both cell lines have similar rates of proliferation.

To determine whether the knockdown of human TDP1 results in an increased sensitivity to ETO, we performed the colony formation assay (Fig. 1E). The IC50 values of HeLa NS cells exposed to ETO were in the range of wild-type HeLa cells reported previously in the literature [33]. The analysis of the IC50 showed that TDP1^{kd} cells are 1.7 times hypersensitive to ETO compared to NS ($p = 0.0386$). In comparison, the IC50 of the Top1 inhibitor camptothecin (CPT) was 2.2 times higher in TDP1^{kd} ($p = 0.0252$, Supplementary Fig. S1B).

3.2. Lack of TDP1 induces accumulation of ETO-stabilized Top2 α cc and alters its removal kinetics

The main activity of Top2 α is to relax supercoiled double stranded DNA by cleaving the backbone of DNA and forming a transient tyrosyl-DNA cleavage complex intermediate, which is stabilized by Top2 poisons.

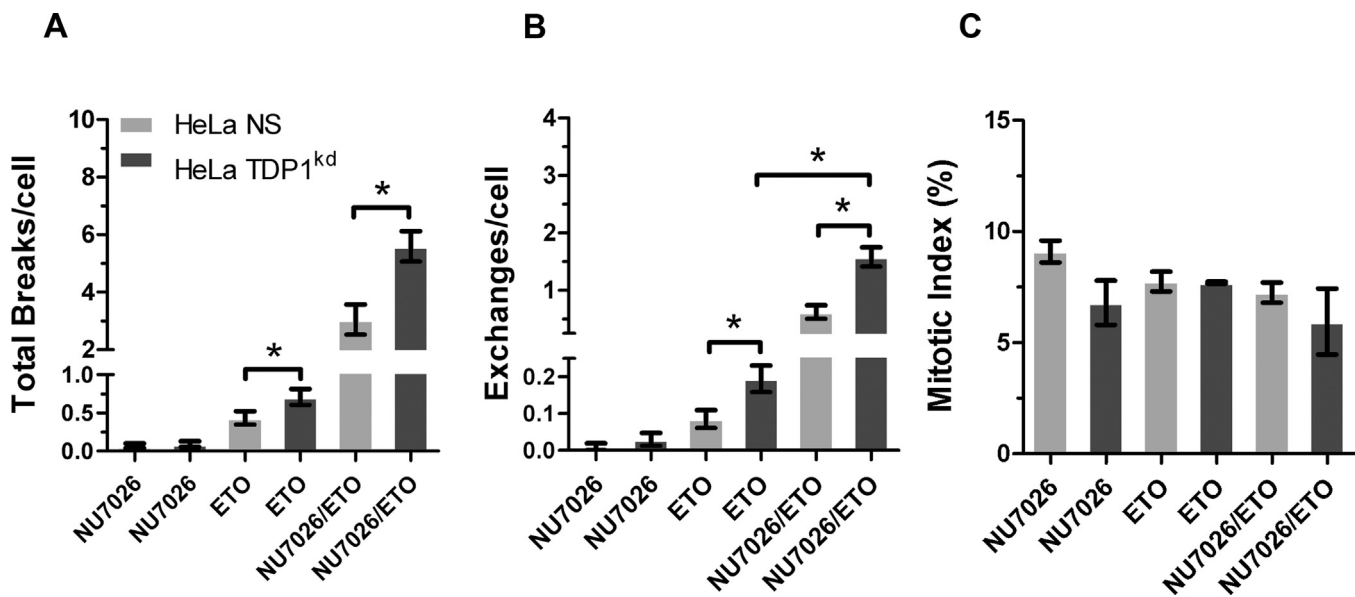


Fig. 5. TDP1 is involved in both C-NHEJ and A-EJ repair events of Top2-mediated DNA DSB. (A) Increased total DNA breaks induced by ETO 1 μ g/ml for 2 h in TDP1 depleted cells pre-treated or not with the DNA-PKcs inhibitor NU7026 10 μ M by 1 h. NU7026 was present in the media during the whole culture time. (B) TDP1 depleted cells showed increased frequencies of misrepair events (chromatid and chromosome exchanges) in the presence or not of NU7026. (C) Mitotic index analyses of TDP1^{kd} and NS cells pre-treated or not with NU7026 and treated with ETO 1 μ g/ml for 2 h. * p <0.05 (Student *t*-test). Error bars indicate s.e.m.

Top2 denaturation/degradation has been reported to be necessary for the repair of stabilized Top2cc [12], although proteasome-independent processing has also been reported [34]. We decided to examine by the DRT assay whether TDP1 might participate in the removal of ETO-stabilized Top2 α cc in a chromatin context in HeLa NS and TDP1^{kd} cells (Fig. 2A). It is relevant to note that an extensive degradation of Top2 α adducts might interfere with the antibody detection.

The cells were analyzed 1 h post-treatment with different ETO doses (Fig. 2B) or following different recovery times in drug-free complete media (Fig. 2C). As seen in Fig. 2B and C (and also in Supplementary Fig. S1C), HeLa TDP1^{kd} accumulated higher amounts of ETO-stabilized Top2 α cc during the 60 min exposure time. This phenomenon was not observed after 30 min exposure, when Top2 α cc levels were similar in both cell lines (data not shown). The frequency distribution of the Top2 α cc intensity of fluorescence from NS and TDP1^{kd} cells are represented in Supplementary Fig. S2A and B, respectively. The increased accumulation of Top2 α cc correlated with diminished amounts of γ H2AX signals (Fig. 2D) in HeLa TDP1^{kd} cells compared to NS. In addition, HeLa TDP1^{kd} had an altered kinetics of removal of Top2 α cc as compared to NS. This was evidenced by a slower removal rate at initial recovery times in TDP1^{kd} (25% more signals), though returning to similar rates of NS at 60 min of recovery (Fig. 2C).

3.3. Late, but not early DSB signaling response, is altered in human cells lacking TDP1

To determine whether TDP1 knockdown cells differ in the signaling steps following ETO-induced DNA DSB formation, HeLa NS and TDP1^{kd} cells were treated for 2 h with ETO and analyzed by western blot for the activation of several DNA damage response proteins. As shown in Fig. 3A, the activation of pS1981ATM, pS2056DNA-PKcs, and the distal transducer pT68CHK2 occurred at similar levels, showing no apparent differences in both cell lines. No detectable activation of pS428ATR was evidenced in both cell lines. However, TDP1^{kd} cells showed an increased activation of

pS296CHK1 (Fig. 3A and B). CHK1 is phosphorylated at multiple sites in response to DNA damage by the kinases ATM/ATR, including Ser317 and Ser345, then resulting in the autophosphorylation of Ser296, which has been associated to the kinase activity of the enzyme and the induction of a G2/M checkpoint [35,36]. TDP1 has been previously shown to physically interact with ATM [37,38]. This prompted us to investigate whether the absence of TDP1 may influence the kinase activity of ATM on the phosphorylation levels of CHK1 following Top2-mediated DNA damage. In order to determine whether CHK1 activation in response to ETO is dependent on ATM, we pre-incubated both cell lines with KU55933, a known inhibitor of ATM kinase activity. On the other hand, to analyze a direct involvement of ATM on the phosphorylation of Ser296 of CHK1, we pre-incubated both cell lines with TCS2312, a known inhibitor of the CHK1 kinase activity, to prevent its autophosphorylation. Fig. 3C shows that ETO-induced CHK1 activation is dependent on ATM, however, the different response shown in TDP1^{kd} cells is not.

In order to check whether the increased phosphorylation of CHK1 in TDP1^{kd} cells would be associated to increased DNA damage signaling, we evaluated the induction of γ H2AX. As shown in Fig. 3D, and in contrast to a shorter exposure, a 2 h treatment with ETO resulted in an increased accumulation of γ H2AX in TDP1^{kd} cells compared with NS.

These results suggest that late, but not early Top2-induced DSB signaling, is altered in TDP1^{kd} cells, as a result of increased DSB formation.

3.4. TDP1 knockdown impairs the repair of Top2-induced DNA DSB

To test whether TDP1 participates in the repair of ETO-mediated DNA DSB, we analyzed the induction of structural chromosome aberrations on HeLa TDP1^{kd} and NS cells following treatment with different doses of ETO (Table S1 and Supplementary Fig. S1D). Fig. 4A shows that the level of total chromosome breaks per cell induced by ETO 1 μ g/ml was significantly increased in HeLa TDP1^{kd} compared with NS. However, there was no difference in those induced

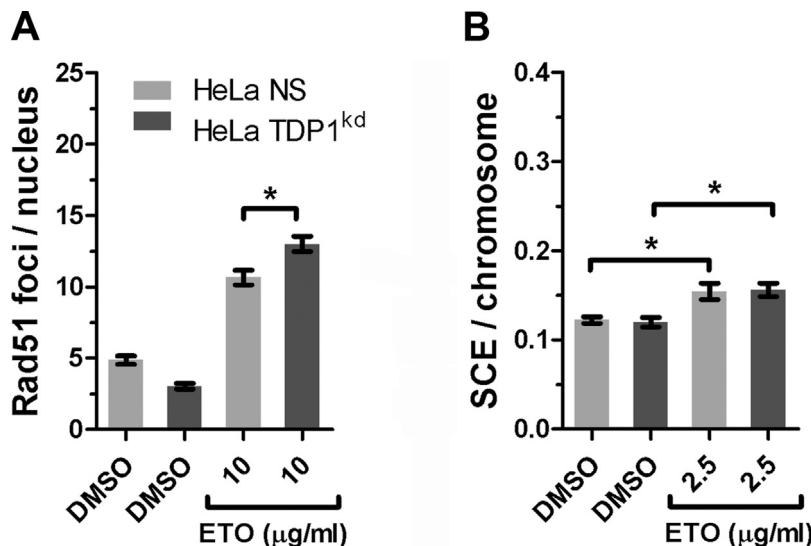


Fig. 6. TDP1 does not alter the HR repair outcome in response to the Top2-induced DNA damage. (A) Rad51 foci formation is increased in HeLa TDP1^{kd} cells in response to ETO. (B) Top2-mediated DSB increased the levels of sister chromatid exchanges (SCE) at a similar extent in both HeLa NS and TDP1^{kd} cells. * $p < 0.05$ (Student *t*-test). Error bars indicate s.e.m.

by ETO 2.5 $\mu\text{g}/\text{ml}$. The analysis of the MI (Fig. 4B) showed that while both cell lines treated with ETO 1 $\mu\text{g}/\text{ml}$ exhibit similar number of mitotic cells, ETO 2.5 $\mu\text{g}/\text{ml}$ reduced significantly the amount of mitotic cells in HeLa TDP1^{kd} compared to NS. Fig. 4C shows the breakage susceptibility index for both cell lines, which mirrors that HeLa TDP1^{kd} accumulates more DNA DSB than NS following exposure to ETO.

Together, these results suggest that TDP1 promotes genome stability by participating in the repair of Top2-induced DNA DSB.

3.5. TDP1 participates in the repair by C-NHEJ and A-EJ of Top2-mediated DNA damage

In order to evaluate the role of TDP1 in the repair of Top2-mediated DSB, we analyzed chromosome spreads from HeLa TDP1^{kd} or NS cells following treatment with ETO in the presence or not of the inhibitor of DNA-PKcs, NU7026 (Table S2). As shown in Fig. 5A (also in Fig. 4A), total chromosome breaks per cell were higher in HeLa TDP1^{kd} than NS cells in response to ETO 1 $\mu\text{g}/\text{ml}$. Similarly, an increased accumulation of chromatid and chromosome exchanges (Fig. 5B) resulting from misrepair events, were shown in HeLa TDP1^{kd} cell line compared to NS. As this dose of ETO is not expected to produce amounts of DSB that can exceed the repair ability of the canonical NHEJ (C-NHEJ), these results argues that TDP1 participates in this repair pathway.

It is known that either when key components of the C-NHEJ are lacking or when it is overwhelmed by high amounts of DSB, the activity of an alternative end joining (A-EJ) pathway is stimulated [39]. As shown in Fig. 5A, the total breaks per cell induced by ETO are still higher in TDP1^{kd} than NS cells when pre-incubated with NU7026. Notice that NU7026 had a slight, although not statistically significant effect on the MI of TDP1^{kd} cell line (Fig. 5C). TDP1 might also contribute to the A-EJ pathway. Therefore, we argued that whether TDP1 contributes to A-EJ, the chromatid and chromosome exchanges per cell in TDP1 depleted cells pre-incubated with NU7026 (TDP1^{kd}, NU7026/ETO treatment) should exceed those found on either NS cells pre-incubated with NU7026 (NS, NU7026/ETO treatment) or cells just lacking TDP1 (TDP1^{kd}, ETO treatment). Thus, the results shown in Fig. 5B also suggest a role of TDP1 in the A-EJ.

Overall, our results support an involvement of TDP1 in both the C-NHEJ and A-EJ process of DSB repair.

3.6. Lack of TDP1 does not affect the HR repair rates of Top2-mediated DSB

To test the participation of TDP1 in the ETO-induced DSB repair by HR, we scored in HeLa TDP1^{kd} and NS the formation of Rad51 nuclear foci 3 h after a 2 h treatment with ETO. As shown in Fig. 6A, ETO-induced Rad51 foci formation is mildly, although significantly increased in HeLa TDP1^{kd} cell line.

In order to determine whether the increased number of Rad51 nuclear foci induced by ETO results in an increased number of HR events, we analyzed the induction of sister chromatid exchanges (SCE). SCE represent the cytological manifestation of an ended Rad51-dependent HR process. As depicted in Fig. 6B, ETO induced an increase in SCE in both cell lines but at similar levels. Therefore, the increased number of Rad51 foci in HeLa TDP1^{kd} may reflect abortive HR repair events.

Together, our results demonstrate that in the absence of TDP1 the HR repair rates of Top2-mediated DNA DSB are not altered.

3.7. TDP1 promotes genome stability following Top2-mediated DNA DSB formation

To check whether genome instability following Top2-mediated DNA DSB is stimulated by TDP1 knockdown, we analyzed the presence of micronuclei (MN) containing γH2AX signals and cells harboring γH2AX signals in their main nuclei in HeLa TDP1^{kd} and NS cells at different times following a 2 h treatment with ETO 2.5 $\mu\text{g}/\text{ml}$. As shown in Fig. 7A, ETO increased similarly the percentage of cells with MN showing γH2AX signals at 20 h post-treatment in both cell lines. However, at the same time, the frequency of cells showing γH2AX positive staining signals in the main nucleus was also increased but was significantly higher in HeLa TDP1^{kd} compared to NS cells (Fig. 7B).

The analyses at 36 h post-treatment (Fig. 7C) still showed increased frequencies of cells with MN containing γH2AX signals, being significantly higher in HeLa TDP1^{kd} compared to NS cells. However, at this time point, just the ETO-treated TDP1^{kd} cells

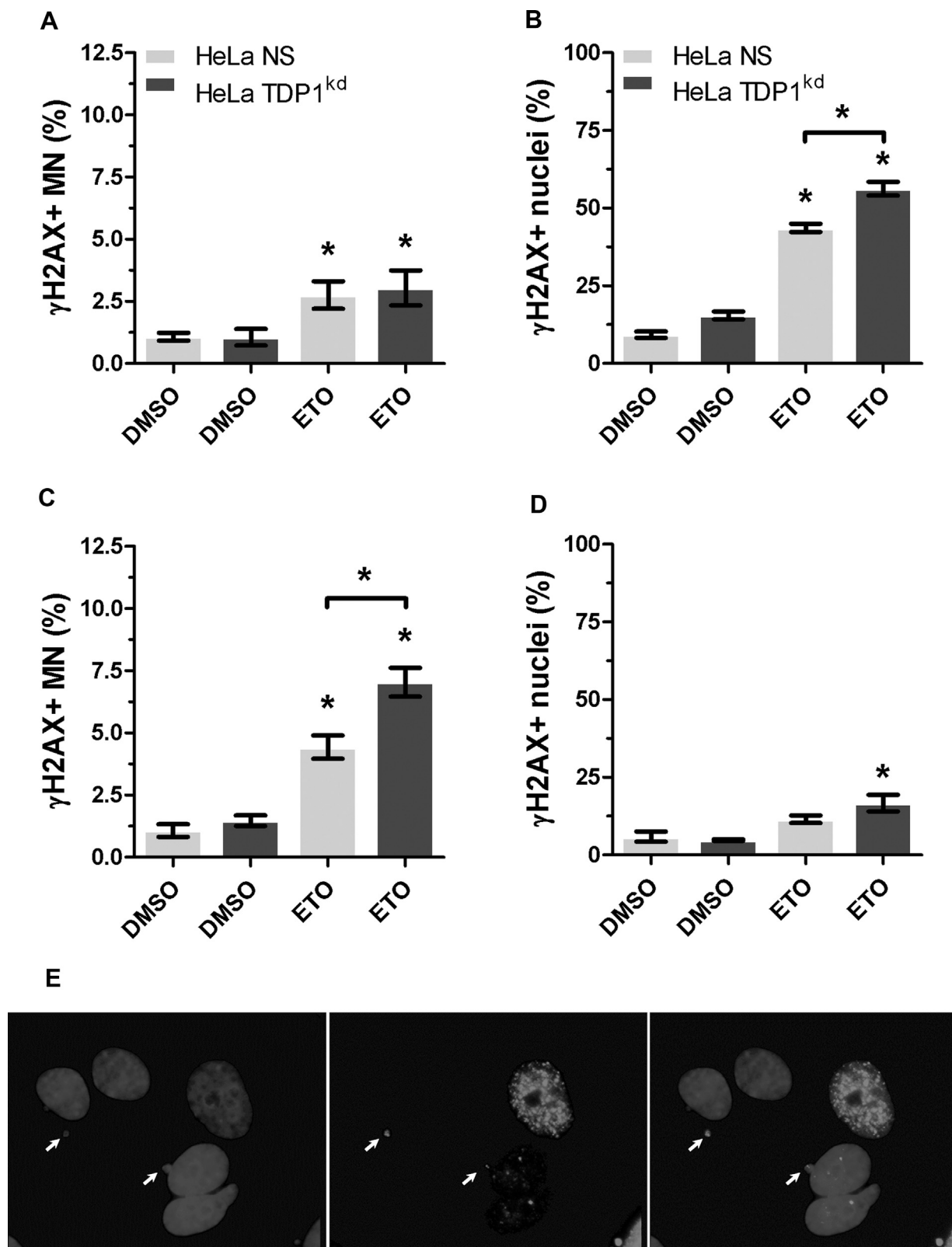


Fig. 7. TDP1 depletion causes genome instability following Top2-mediated DNA damage in HeLa cells. (A) Similar levels of micronuclei (MN) containing γ H2AX signals are found in HeLa TDP1^{kd} and NS cells 20 h after a 2 h treatment with ETO 2.5 μ g/ml. (B) At the same time, a significant increase in the levels of nuclei containing γ H2AX foci is found in HeLa TDP1^{kd} cells. (C) At 36 h post-treatment, the levels of MN γ H2AX+ raised in TDP1^{kd} cells compared to NS. (D) While nucleus containing γ H2AX foci diminished in both cell lines at this time, an increased number of them remained in TDP1^{kd} cells. (E) Representative images of MN containing γ H2AX+ signals (white arrows) and a nucleus containing γ H2AX foci in HeLa TDP1^{kd} cells at 36 h post-treatment with ETO. * $p < 0.05$ (Student *t*-test). Error bars indicate s.e.m.

retained significantly increased amounts of nucleus with γ H2AX signals compared to NS cells (Fig. 7D and E). This may be due to a higher number of TDP1kd cells that remained arrested by a G2 checkpoint.

Overall, our data show that in response to ETO-induced DNA DSB, TDP1 depletion diminish the DNA repair efficiency impacting on the maintenance of the genome integrity.

4. Discussion

The removal of abortive Top2 α cc is a fundamental task to avoid the collision of the replication fork and the transcriptional machinery [34], which may result in the generation of persistent DNA DSB. These lesions are the main responsible for cytotoxicity induced by several chemotherapeutic agents that acts as Top2 poisons [40,41].

TDP1 is a DNA repair enzyme which has been demonstrated to hydrolyze several covalent adducts from DNA, including dead-end complexes Top1-DNA. The role of TDP1 in the removal of Top1 cleavage complexes has been reported from yeast to humans [24,42]; however, its activity in the removal of Top2cc is still unresolved. Biochemical studies using different double stranded oligonucleotide substrates and TDP1 partially purified failed to detect a 5' tyrosyl-phosphodiesterase activity [25,43,44]. Conversely, 5' tyrosyl-double stranded oligonucleotide substrates with 4-base overhangs, similar to those resulting from Top2 cleavage, were efficiently processed by human recombinant TDP1 [22]. Therefore, the kind of substrate and/or the origin of the enzyme seem to affect the activity of TDP1. Moreover, human SCAN1 mutant lymphoblastoid cell lines, TDP1 knock out mice and embryonic fibroblasts did not show hypersensitivity to ETO [21,24,45]. However, overexpression of TDP1 in human cells diminished the DNA damage induced by ETO [28]. A more difficult interpretation can be made from data derived from chicken TDP1 $^{−/−}$ DT40 cell lines, where hypersensitivity to ETO was shown [22,29] although opposed results were also reported [27].

Here we show that TDP1 knockdown in human proliferating cells confers hypersensitivity to ETO. Moreover, the lack of TDP1 resulted in an accumulation of ETO-stabilized Top2 α cc, which were then efficiently removed by TDP1-independent mechanisms. In this regard, the recently discovered 5'-tyrosyl phosphodiesterase activity of the TDP2 enzyme has been reported in human cells [44,46], although other endonucleases have also been implicated in removing covalently bound Top2 [47]. Structural data suggest that TDP2 may require unfolding or proteolytic processing of Top2 to access the DNA substrate [48]. Biochemical data suggested that TDP1 cannot remove full-length Top1 from DNA, requiring a previous denaturation or proteolytic degradation [25,43,49]. However, the ability of TDP1 to remove Top2 α cc remains controversial. The current view of the DNA end processing following abortive Top2cc formation assume that sumoylation and/or ubiquitination-dependent proteolysis is required to remove a Top2-peptide bound from 5' DNA termini [50]. It is interesting to note that even though proteasome inhibition is carried out previous to Top2 poisoning, a significant higher amount of γ H2AX signals are still developed at short exposure times (data not shown) [12,51], suggesting that proteolysis-independent mechanisms may also co-exist. Moreover, a recent report [34] showed that after exposure to low dose of ETO, similar to doses used in our study, the development of DSB signals were insensitive to proteasome inhibition. This study also determined that under low dose treatments with ETO, Top2 α is the major responsible for the induction of replication-dependent DSB. Our data showed an increased accumulation of Top2 α cc in TDP1kd cells, which combined with a diminished appearance of γ H2AX signals, suggest an involvement of TDP1 in the removal of Top2 α cc.

It has been shown that TDP1 interacts with several DDR factors [37,52]. In response to Top1 poisons, ATM and DNA-PKcs phosphorylate TDP1 on Ser81, which confers more stability to the molecule, enabling its association with XRCC1 and potentiating its mobilization to DNA damaged sites [37]. Since the depletion of TDP1 might also impact in the DNA DSB damage signaling, we analyzed the activation of several DDR proteins up- and downstream the induction of γ H2AX. Our data show that neither the activation of proximal transducers, nor the induction of the distal transducer CHK2 is altered by depletion of TDP1. Interestingly, an increased accumulation of pS296CHK1 in response to ETO was shown in TDP1 depleted cells. No regulatory effect of TDP1 depletion was found to modulate direct- or indirectly the phosphorylation of CHK1. Instead, a time-dependent increased accumulation of γ H2AX was found to correlate with the increased phosphorylation on Ser296 of CHK1.

Here we show that depletion of TDP1 alters the DSB repair ability following Top2-mediated DNA DSB. While the ETO-induced HR repair rates did not seem to be altered by the depletion of TDP1, the evidenced increase of chromatid and chromosome breaks and exchanges after treatment with ETO supports a role of TDP1 in the C-NHEJ pathway.

Early work showed that following IR, an impaired DNA-PKcs activity stimulates a slow A-EJ form of DSB repair [53]. Here we show that inhibiting DNA-PKcs activity on TDP1 depleted cells lead to a higher incidence of misrepair events in response to ETO, which should not be expected unless TDP1 may also have a role in the A-EJ. Interestingly, it has recently been reported a direct interaction of the regulatory N-terminal domain of TDP1 with the catalytic domain of PARP-1, resulting in the PARylation and stabilization of TDP1 in response to Top1cc-induced DNA damage; and the recruitment of TDP1 and XRCC1 to the damaged sites [54]. In addition, other evidence showed that phosphorylation of TDP1 on Ser81 promotes the interaction of TDP1 with Ligase III α [55]. As there is evidence that PARP-1, XRCC1 and Ligase III α proteins have a role on A-EJ [56], it is likely that a platform for TDP1 activity in this pathway may also be mounted in response to Top2-mediated DNA damage.

Regardless of which DSB repair pathways are impaired by TDP1 depletion, here we show that genome stability is compromised as evidenced by the increase of micronuclei containing γ H2AX signals following Top2-induced DSB.

In summary, our results show that in human proliferating cells TDP1 participates in the removal of Top2 α cc, though its activity may be replaced by alternative mechanisms. However, its depletion impairs the repair ability of Top2-induced DSB by disturbing both C-NHEJ and A-EJ; and thus, promoting genomic instability but also hypersensitivity. Further studies should determine whether combined therapies of Top2 poisons with chemical inhibitors of TDP1 may result in any advantage for cancer treatment.

Conflict of interest

The authors declare that there are no conflicts of interest.

Acknowledgments

This study was supported with grants from Fundación Alberto J. Roemmers 2013 and PICT-1230 from Agencia Nacional de Promoción Científica y Tecnológica to MdCN. The funders had no role in study design, data collection and analysis, decision to publish, or preparation of the manuscript.

We thank Dr. V. I. Landoni for critical revision of the manuscript. We also thank Dr. N. Galassi, N. Riera and M. Filippo for helping us with flow cytometry experiments.

Appendix A. Supplementary data

Supplementary data associated with this article can be found, in the online version, at <http://dx.doi.org/10.1016/j.mrfmmm.2015.09.003>.

References

- [1] J. Roca, Topoisomerase II a fitted mechanism for the chromatin landscape, *Nucl. Acids Res.* 37 (2009) 721–730.
- [2] M.M. Heck, W.N. Hittelman, W.C. Earnshaw, Differential expression of DNA topoisomerases I and II during the eukaryotic cell cycle, *Proc. Natl. Acad. Sci. U. S. A.* 85 (1988) 1086–1090.
- [3] G. Capranico, S. Tinelli, C.A. Austin, M.L. Fisher, F. Zunino, Different patterns of gene expression of topoisomerase II isoforms in differentiated tissues during murine development, *Biochim. Biophys. Acta* 1132 (1992) 43–48.
- [4] Y. Pommier, E. Leo, H. Zhang, C. Marchand, DNA topoisomerases and their poisoning by anticancer and antibacterial drugs, *Chem. Biol.* 17 (2010) 421–433.
- [5] P.S. Kingma, C.A. Greider, N. Osheroff, Spontaneous DNA lesions poison human topoisomerase IIalpha and stimulate cleavage proximal to leukemic 11q23 chromosomal breakpoints, *Biochemistry* 36 (1997) 5934–5939.
- [6] M. Sabourin, N. Osheroff, Sensitivity of human type II topoisomerases to DNA damage: stimulation of enzyme-mediated DNA cleavage by abasic, oxidized and alkylated lesions, *Nucl. Acids Res.* 28 (2000) 1947–1954.
- [7] A.M. Wilstermann, N. Osheroff, Base excision repair intermediates as topoisomerase II poisons, *J. Biol. Chem.* 276 (2001) 46290–46296.
- [8] M. Bigioni, F. Zunino, G. Capranico, Base mutation analysis of topoisomerase II–idarubicin-DNA ternary complex formation. Evidence for enzyme subunit cooperativity in DNA cleavage, *Nucl. Acids Res.* 22 (1994) 2274–2281.
- [9] A.H. Corbett, E.L. Zechiedrich, R.S. Lloyd, N. Osheroff, Inhibition of eukaryotic topoisomerase II by ultraviolet-induced cyclobutane pyrimidine dimers, *J. Biol. Chem.* 266 (1991) 19666–19671.
- [10] P.S. Kingma, D.A. Burden, N. Osheroff, Binding of etoposide to topoisomerase II in the absence of DNA: decreased affinity as a mechanism of drug resistance, *Biochemistry* 38 (1999) 3457–3461.
- [11] S.D. Cline, N. Osheroff, Cytosine arabinoside lesions are position-specific topoisomerase II poisons and stimulate DNA cleavage mediated by the human type II enzymes, *J. Biol. Chem.* 274 (1999) 29740–29743.
- [12] A. Zhang, Y.L. Lyu, C.P. Lin, N. Zhou, A.M. Azarova, et al., A protease pathway for the repair of topoisomerase II-DNA covalent complexes, *J. Biol. Chem.* 281 (2006) 35997–36003.
- [13] J.L. Nitiss, Targeting DNA topoisomerase II in cancer chemotherapy, *Nat. Rev. Cancer* 9 (2009) 338–350.
- [14] S. Karanika, T. Karantanou, L. Li, P.G. Corn, T.C. Thompson, DNA damage response and prostate cancer: defects, regulation and therapeutic implications, *Oncogene* 34 (2014) 1815–1822.
- [15] Y. Chen, R.Y. Poon, The multiple checkpoint functions of CHK1 and CHK2 in maintenance of genome stability, *Front. Biosci. J. Virtual Libr.* 13 (2008) 5016–5029.
- [16] M. Jasin, R. Rothstein, Repair of strand breaks by homologous recombination, *Cold Spring Harb. Perspect. Biol.* 5 (2013) a012740.
- [17] M.R. Lieber, The mechanism of human nonhomologous DNA end joining, *J. Biol. Chem.* 283 (2008) 1–5.
- [18] G. Iliakis, Backup pathways of NHEJ in cells of higher eukaryotes: cell cycle dependence, *Radiat. Oncol.* 92 (2009) 310–315.
- [19] D. Simsek, M. Jasin, Alternative end-joining is suppressed by the canonical NHEJ component Xrcc4-ligase IV during chromosomal translocation formation, *Nat. Struct. Mol. Biol.* 17 (2010) 410–416.
- [20] B.B. Das, T.S. Dexheimer, K. Maddali, Y. Pommier, Role of tyrosyl-DNA phosphodiesterase (TDP1) in mitochondria, *Proc. Natl. Acad. Sci. U. S. A.* 107 (2010) 19790–19795.
- [21] R. Hirano, H. Interthal, C. Huang, T. Nakamura, K. Deguchi, et al., Spinocerebellar ataxia with axonal neuropathy: consequence of a Tdp1 recessive neomorphic mutation? *EMBO J.* 26 (2007) 4732–4743.
- [22] J. Murai, S.Y. Huang, B.B. Das, T.S. Dexheimer, S. Takeda, et al., Tyrosyl-DNA phosphodiesterase 1 (TDP1) repairs DNA damage induced by topoisomerases I and II and base alkylation in vertebrate cells, *J. Biol. Chem.* 287 (2012) 12848–12857.
- [23] M. Alagoz, O.S. Wells, S.F. El-Khamisy, TDP1 deficiency sensitizes human cells to base damage via distinct topoisomerase I and PARP mechanisms with potential applications for cancer therapy, *Nucl. Acids Res.* 42 (2014) 3089–3103.
- [24] H. Interthal, H.J. Chen, T.E. Kehl-Fie, J. Zottmann, J.B. Leppard, et al., SCAN1 mutant Tdp1 accumulates the enzyme-DNA intermediate and causes camptothecin hypersensitivity, *EMBO J.* 24 (2005) 2224–2233.
- [25] H. Interthal, H.J. Chen, J.J. Champoux, Human Tdp1 cleaves a broad spectrum of substrates, including phosphoamido linkages, *J. Biol. Chem.* 280 (2005) 36518–36528.
- [26] K.C. Nitiss, M. Malik, X. He, S.W. White, J.L. Nitiss, Tyrosyl-DNA phosphodiesterase (Tdp1) participates in the repair of Top2-mediated DNA damage, *Proc. Natl. Acad. Sci. U. S. A.* 103 (2006) 8953–8958.
- [27] Z. Zeng, A. Sharma, L. Ju, J. Murai, L. Umans, et al., TDP2 promotes repair of topoisomerase I-mediated DNA damage in the absence of TDP1, *Nucl. Acids Res.* 40 (2012) 8371–8380.
- [28] H.U. Barthelmes, M. Habermeyer, M.O. Christensen, C. Mielke, H. Interthal, et al., TDP1 overexpression in human cells counteracts DNA damage mediated by topoisomerases I and II, *J. Biol. Chem.* 279 (2004) 55618–55625.
- [29] Y. Maede, H. Shimizu, T. Fukushima, T. Kogame, T. Nakamura, et al., Differential and common DNA repair pathways for topoisomerase I- and II-targeted drugs in a genetic DT40 repair cell screen panel, *Mol. Cancer Ther.* 13 (2014) 214–220.
- [30] M.W. Pfaffl, A new mathematical model for relative quantification in real-time RT-PCR, *Nucl. Acids Res.* 29 (2001) e45.
- [31] M. Bradford, A rapid and sensitive method for the quantitation of microgram quantities of protein utilizing the principle of protein-dye binding, *Anal. Biochem.* 72 (1976) 248–254.
- [32] M. Agostinho, J. Rino, J. Braga, F. Ferreira, S. Steffensen, et al., Human topoisomerase IIalpha: targeting to subchromosomal sites of activity during interphase and mitosis, *Mol. Biol. Cell* 15 (2004) 2388–2400.
- [33] M.J. Elliott, L. Stribinskiene, R.B. Lock, Expression of Bcl-2 in human epithelial tumor (HeLa) cells enhances clonogenic survival following exposure to 5-fluoro-2'-deoxyuridine or staurosporine, but not following exposure to etoposide or doxorubicin, *Cancer Chemother. Pharmacol.* 41 (1998) 457–463.
- [34] M. Tammaro, P. Barr, B. Ricci, H. Yan, Replication-dependent and transcription-dependent mechanisms of DNA double-strand break induction by the topoisomerase 2-targeting drug etoposide, *PLoS One* 8 (2013) e79202.
- [35] Y. Dai, S. Grant, New insights into checkpoint kinase 1 in the DNA damage response signaling network, *Clin. Cancer Res.* 16 (2010) 376–383.
- [36] N. Okita, S. Minato, E. Ohmi, S. Tanuma, Y. Higami, DNA damage-induced CHK1 autophosphorylation at Ser296 is regulated by an intramolecular mechanism, *FEBS Lett.* 586 (2012) 3974–3979.
- [37] B.B. Das, S. Antony, S. Gupta, T.S. Dexheimer, C.E. Redon, et al., Optimal function of the DNA repair enzyme TDP1 requires its phosphorylation by ATM and/or DNA-PK, *EMBO J.* 28 (2009) 3667–3680.
- [38] J.J. Mu, Y. Wang, H. Luo, M. Leng, J. Zhang, et al., A proteomic analysis of ataxia telangiectasia-mutated (ATM)/ATM-Rad3-related (ATR) substrates identifies the ubiquitin-proteasome system as a regulator for DNA damage checkpoints, *J. Biol. Chem.* 282 (2007) 17330–17334.
- [39] M.R. Lieber, NHEJ and its backup pathways in chromosomal translocations, *Nat. Struct. Mol. Biol.* 17 (2010) 393–395.
- [40] M. de Campos-Nebel, I. Larripa, M. Gonzalez-Cid, Topoisomerase II-mediated DNA damage is differently repaired during the cell cycle by non-homologous end joining and homologous recombination, *PLoS One* 5 (2010) e12541.
- [41] M. Pendleton, R.H. Lindsey Jr., C.A. Felix, D. Grimwade, N. Osheroff, Topoisomerase II and leukemia, *Ann. N. Y. Acad. Sci.* 1310 (2014) 98–110.
- [42] J.J. Pouliot, K.C. Yao, C.A. Robertson, H.A. Nash, Yeast gene for a Tyr-DNA phosphodiesterase that repairs topoisomerase I complexes, *Science* 286 (1999) 552–555.
- [43] S.W. Yang, A.B. Burgin Jr., B.N. Huizenga, C.A. Robertson, K.C. Yao, et al., A eukaryotic enzyme that can disjoin dead-end covalent complexes between DNA and type I topoisomerases, *Proc. Natl. Acad. Sci. U. S. A.* 93 (1996) 11534–11539.
- [44] F. Cortes Ledesma, S.F. El Khamisy, M.C. Zuma, K. Osborn, K.W. Caldecott, A human 5'-tyrosyl DNA phosphodiesterase that repairs topoisomerase-mediated DNA damage, *Nature* 461 (2009) 674–678.
- [45] Z.H. Miao, K. Agama, O. Sordet, L. Povirk, K.W. Kohn, et al., Hereditary ataxia SCAN1 cells are defective for the repair of transcription-dependent topoisomerase I cleavage complexes, *DNA Repair* 5 (2006) 1489–1494.
- [46] F. Gomez-Herreros, R. Romero-Granados, Z. Zeng, A. Alvarez-Quilon, C. Quintero, et al., TDP2-dependent non-homologous end-joining protects against topoisomerase II-induced DNA breaks and genome instability in cells and in vivo, *PLoS Genet.* 9 (2013) e1003226.
- [47] K. Nakamura, T. Kogame, H. Oshima, A. Shinohara, Y. Sumitomo, et al., Collaborative action of Brca1 and CtIP in elimination of covalent modifications from double-strand breaks to facilitate subsequent break repair, *PLoS Genet.* 6 (2010) e1000828.
- [48] M.J. Schellenberg, C.D. Appel, S. Adhikari, P.D. Robertson, D.A. Ramsden, et al., Mechanism of repair of 5'-topoisomerase II-DNA adducts by mammalian tyrosyl-DNA phosphodiesterase 2, *Nat. Struct. Mol. Biol.* 19 (2012) 1363–1371.
- [49] H. Interthal, J.J. Champoux, Effects of DNA and protein size on substrate cleavage by human tyrosyl-DNA phosphodiesterase 1, *Biochem. J.* 436 (2011) 559–566.
- [50] K.W. Caldecott, Tyrosyl DNA phosphodiesterase 2, an enzyme fit for purpose, *Nat. Struct. Mol. Biol.* 19 (2012) 1212–1213.
- [51] Y.L. Lyu, J.E. Kerrigan, C.P. Lin, A.M. Azarova, Y.C. Tsai, et al., Topoisomerase IIbeta mediated DNA double-strand breaks: implications in doxorubicin cardiotoxicity and prevention by dextrazoxane, *Cancer Res.* 67 (2007) 8839–8846.
- [52] S.F. El-Khamisy, G.M. Saifi, M. Weinfeld, F. Johansson, T. Helleday, et al., Defective DNA single-strand break repair in spinocerebellar ataxia with axonal neuropathy-1, *Nature* 434 (2005) 108–113.

- [53] R. Perrault, H. Wang, M. Wang, B. Rosidi, G. Iliakis, Backup pathways of NHEJ are suppressed by DNA-PK, *J. Cell. Biochem.* 92 (2004) 781–794.
- [54] B.B. Das, S.Y. Huang, J. Murai, I. Rehman, J.C. Ame, et al., PARP1-TDP1 coupling for the repair of topoisomerase I-induced DNA damage, *Nucl. Acids Res.* 42 (2014) 4435–4449.
- [55] S.C. Chiang, J. Carroll, S.F. El-Khamisy, TDP1 serine 81 promotes interaction with DNA ligase IIIalpha and facilitates cell survival following DNA damage, *Cell Cycle* 9 (2010) 588–595.
- [56] A. Soni, M. Siemann, M. Grabos, T. Murmann, G.E. Pantelias, et al., Requirement for Parp-1 and DNA ligases 1 or 3 but not of Xrcc1 in chromosomal translocation formation by backup end joining, *Nucl. Acids Res.* 42 (2014) 6380–6392.